ACS Medicinal Chemistry Letters
Cite This: ACS Med. Chem. Lett. XXXX, XXX, XXX−XXX
Letter
pubs.acs.org/acsmedchemlett

Discovery of Potent and Selective MTH1 Inhibitors for Oncology: Enabling Rapid Target (In)Validation

Julie Farand,*[,†] Jeffrey E. Kropf,[‡] Peter Blomgren,[‡] Jianjun Xu,[‡] Aaron C. Schmitt,[‡] Zachary E. Newby,[†] Ting Wang,[†] Eisuke Murakami,[†] Ona Barauskas,[†] Jawahar Sudhamsu,[†] Joy Y. Feng,[†] Anita Niedziela-Majka,[†] Brian E. Schultz,[†] Karen Schwartz,[†] Serge Viatchenko-Karpinski,[†] Dmytro Kornyeyev,[†] Adam Kashishian,[‡] Peidong Fan,[†] Xiaowu Chen,[†] Eric B. Lansdon,[†] Michael O. Ports,[‡] Kevin S. Currie,[‡] William J. Watkins,[†] and Gregory T. Notte[†]

[†]Gilead Sciences, Inc. 333 Lakeside Drive, Foster City, California 94404, United States
[‡]Gilead Sciences, Inc. 199 East Blaine Street, Seattle, Washington 98102, United States

Supporting Information

ABSTRACT: We describe the discovery of three structurally differentiated potent and selective MTH1 inhibitors and their subsequent use to investigate MTH1 as an oncology target, culminating in target (in)validation. Tetrahydronaphthyridine **5** was rapidly identified as a highly potent MTH1 inhibitor (IC_{50} = 0.043 nM). Cocrystallization of **5** with MTH1 revealed the ligand in a Φ-*cis*-*N*-(pyridin-2-yl)acetamide conformation enabling a key intramolecular hydrogen bond and polar interactions with residues Gly34 and Asp120. Modification of literature compound **TH287** with *O*- and *N*-linked aryl and alkyl aryl substituents led to the discovery of potent pyrimidine-2,4,6-triamine **25** (IC_{50} = 0.49 nM). Triazolopyridine **32** emerged as a highly selective lead compound with a suitable *in vitro* profile and desirable pharmacokinetic properties in rat. Elucidation of the DNA damage response, cell viability, and intracellular concentrations of oxo-NTPs (oxidized nucleoside triphosphates) as a function of MTH1 knockdown and/or small molecule inhibition was studied. Based on our findings, we were unable to provide evidence to further pursue MTH1 as an oncology target.

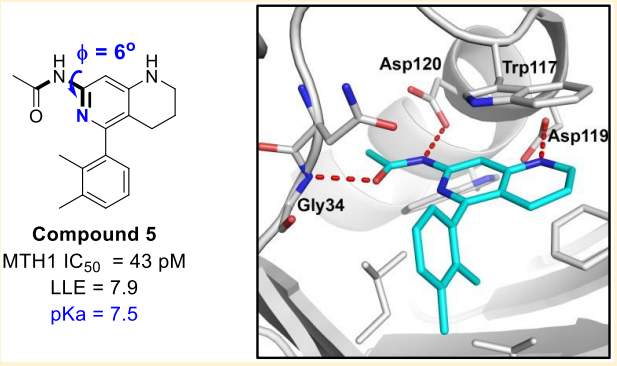

KEYWORDS: *MutT homologue 1(MTH1) inhibition, 8-oxo-dGTP, tetrahydronaphthyridine, triazolopyridine, DNA damage*

In 2018, 59 new molecular entities were approved by the FDA's Center for Drug Evaluation and Research (CDER), 27% of which were developed as oncology therapies (12 new chemical entities and 4 biologics).[1,2] Between 2014 and 2018, cancer drugs consistently achieved the highest number of FDA approvals by therapeutic area, accounting for nearly 25% of all approvals. Addressing the need for safe and effective cancer therapies has been challenging, and prosecuting drug discovery programs for oncology targets requires rigorous preclinical target validation. In 2014, two back-to-back *Nature* publications described MTH1 as cancer phenotypic lethal with great promise as a small molecule targeted therapy for oncology.[3,4] MutT homologue 1 (MTH1 or NUDT1) is a member of the Nudix phosphohydrolase superfamily of enzymes and is a pyrophosphatase that selectively recognizes oxidized purine nucleoside triphosphates, thus converting 8-oxo-dGTP or 2-OH-dATP to 8-oxo-dGMP or 2-OH-dAMP. In normal cells, MTH1 has been described as a sanitizing enzyme capable of preventing the incorporation of oxo-dNTPs into DNA. Cancer cells, however, have an altered redox state with higher levels of reactive oxygen species (ROS) leading to elevated levels of oxidative stress. Disruption of nucleotide pool homeostasis and dysregulation of DNA repair by MTH1 inhibition in tumor cells could increase the incorporation of mismatched oxidized bases into DNA, thus leading to transversion mutations, DNA damage, and cancer cell death.[5] Gad et al.[3] demonstrated that MTH1 inhibition with small molecules **TH287** and **TH588**, or via genetic knockdown, resulted in DNA damage and reduced clonogenic survival and cell viability. Based on these compelling results, we initiated a preclinical research program to evaluate MTH1 as a potential target for oncology. At the onset of our research, only the small molecules shown in Figure 1 were known in the literature to demonstrate biochemical inhibition of MTH1.[3,4,6] When **TH287**, **TH588**, **SCH51344**, and **(*S*)-crizotinib** were profiled in our three-day cell viability assay, we observed discrepancies between their

Special Issue: Women in Medicinal Chemistry

Received: September 12, 2019
Accepted: November 12, 2019

DOI: 10.1021/acsmedchemlett.9b00420
ACS Med. Chem. Lett. XXXX, XXX, XXX−XXX

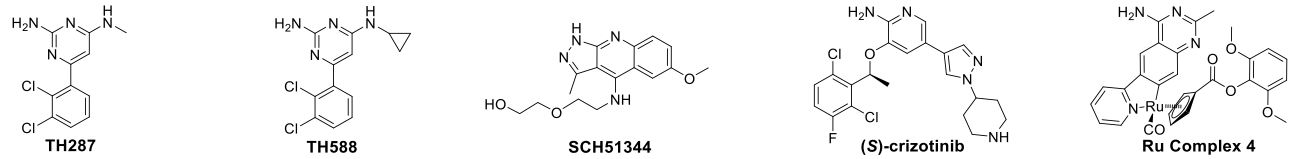

Figure 1. Structures of literature MTH1 inhibitors. Internal biochemical potencies (8-oxo-dGTP as substrate) and three-day cell viability (CellTiter-Glo) in U2OS and SW480 cells are reported (*literature values).

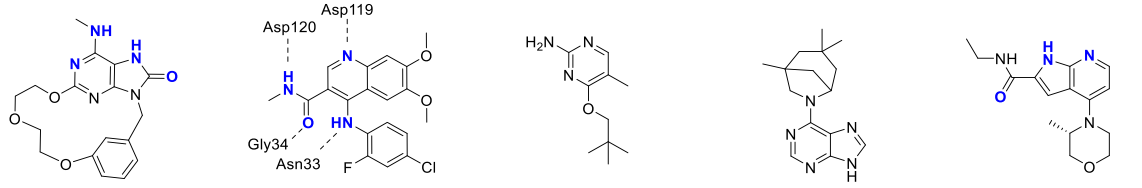

Figure 2. Representative structures of a selection of reported tool compounds used for target validation studies and their MTH1 biochemical potencies (8-oxo-dGTP as substrate). Cocrystal structures of AZ compound **15**,[7] AZ compound **19**,[7] and BAY-707[10] bound to MTH1 (PDB code 5ANU, 5ANV, 5NHY, respectively) revealed hydrogen bond donors and acceptors (blue) engaging Asp119, Asp120, Gly34, and/or Asn33 in the MTH1 active site.

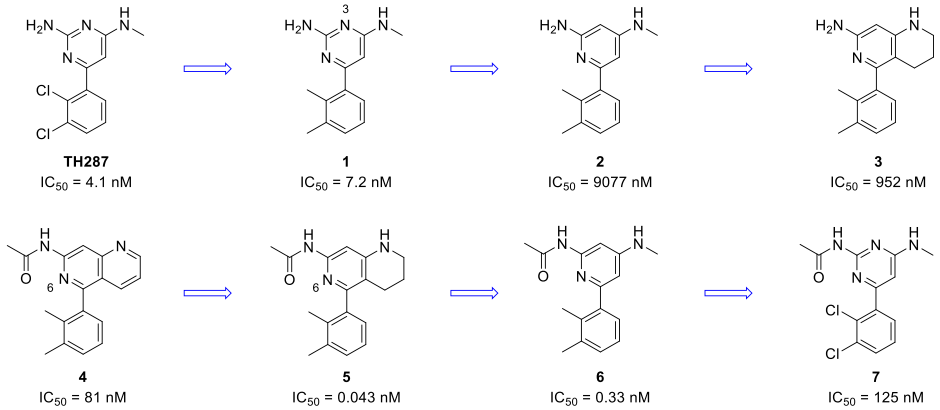

Figure 3. Our initial chemistry efforts yielded highly potent MTH1 inhibitors. For number of replicates and standard error of the mean, see the Supporting Information.

biochemical potencies (nM) and their phenotypic cellular effects (μM) in U2OS and SW480 cell lines. Additionally, Huber et al.[4] had reported that MTH1 overexpression rescued SW480 cells from the cell killing effects of **SCH51344** but not **(*S*)-crizotinib**. Thus, our initial efforts aimed to address these discrepancies by concurrently (1) expressing the full length human MTH1 protein for structural studies, (2) identifying structurally differentiated, selective, and potent small molecule tool compounds, and (3) performing validation studies in shRNA-mediated MTH1 knockdown cell lines.

Several other research groups also initiated MTH1 programs based upon the same literature reports, systematically executed elegant target validation studies, and have since shared their findings.[7−10] Common means to elucidate the cellular effect of MTH1 inhibition included, but are not limited to, thermal stabilization assays to assess target engagement, kinase profiling to evaluate off-target liabilities, cell viability and growth inhibition assays, immunofluorescence/immunoblots of DNA damage response signaling markers, proteomics, cell cycle analysis, and genetic knockdown of MTH1. Importantly, the identification of structurally differentiated MTH1 tool compounds proved to be essential for all studies performed (Figure 2). Herein, we share a similar approach and present the discovery of three potent and selective MTH1 chemotypes, one of which achieved unprecedented levels of biochemical potency (tetrahydronaphthyridine **5**, IC_{50} = 0.043 nM). Furthermore, we share methodology that was developed to measure intracellular concentrations of oxo-NTPs as an *in vitro* biomarker of MTH1 target engagement.

Examination of the published MTH1 cocrystal structures with 8-oxo-dGMP and inhibitors **TH287** and **TH588** revealed common key hydrogen bonding interactions with active site residues Asp119, Asp120, and Asn33.[11,3] After establishing that the 2,3-dichlorophenyl substituent in **TH287** (MTH1 IC_{50} = 4.1 nM) could be replaced with 2,3-dimethylphenyl without significant loss in potency (MTH1 IC_{50} of **1** = 7.2 nM), we set out to further understand the relationship between the nitrogen-mediated hydrogen bonds in the **TH**-series and MTH1 biochemical potency by conducting a series of nitrogen deletions, acetylations, and ring annulations (Figure 3). The >1000-fold loss in potency upon removal of N3 (**2** vs **1**) was suggestive of disruption of a key hydrogen bond. However, one

DOI: 10.1021/acsmedchemlett.9b00420
ACS Med. Chem. Lett. XXXX, XXX, XXX−XXX

order of magnitude in potency was restored upon incorporation of a bicycle in the form of **3**, synthesized as illustrated in Scheme 1. These results prompted us to prepare naphthyridine

Scheme 1. General Synthesis of Tetrahydronaphthyridines[a]

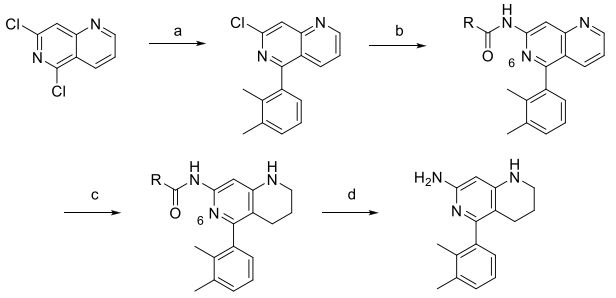

[a]Reagents and conditions: (a) $ArB(OH)_2$, $Pd(PPh_3)_4$, 1,4-dioxane/water (2:1), 80 °C, 1 h, 96%; (b) $RC(O)NH_2$, $Pd_2(dba)_3$, *t*-BuXPhos, Cs_2CO_3, 1,4-dioxane, 100 °C, 18 h, 20−82%; (c) PtO_2, H_2 (40 psi), 4 M HCl in 1,4-dioxane, 15 min, 20−76%; (d) when R = O*t*Bu, TFA/DCM (3:1), rt, 5 h, 12%.

and tetrahydronaphthyridine acetamides **4** and **5** to interrogate the electronic preferences of the ligand's nitrogen atoms with Asp residues 119 and 120. Naphthyridine **4** was moderately potent (MTH1 IC_{50} = 81 nM), while, remarkably, tetrahydronaphthyridine **5** demonstrated a 1800-fold improvement in potency (IC_{50} = 43 pM, LLE = 7.9) relative to **4**. Cocrystallization of **4** with MTH1 revealed key hydrogen bonding interactions with both aspartates, as observed with **TH287**, a $\pi-\pi$ stacking interaction with Trp 117; in making a hydrogen bond to a water molecule, the acetamide of **4** is 23° out of the plane of the aryl system (Figure 4A). Interestingly,

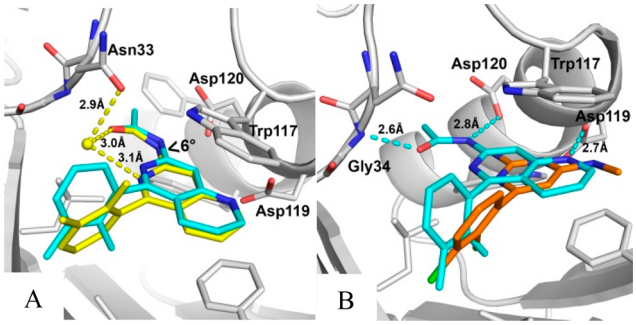

Figure 4. Cocrystal structures of MTH1 with inhibitors. MTH1 (gray) is drawn from the complex with compound **5**. (A) Overlay of **4** (yellow, 1.5 Å, PDB code 6US3) and **5** (cyan) illustrating Φ-*cis* dihedral angles of 23° and 6°, respectively, and the resulting shifts of the 2,3-dimethyphenyl moieties. Unlike tetrahydronaphthyridine **5**, naphthyridine **4** engages Asn33 via a water (yellow sphere)-mediated interaction. (B) Cocrystal structure of **5** (cyan) bound to MTH1 (1.8 Å, PDB code 6US2) showing the shifted register of hydrogen bond interactions relative to TH287 (orange, PDB code 4N1T). No significant changes to the protein were observed between MTH1 complexed to **4** and **5**.

tetrahydronaphthyridine **5** when cocrystallized with MTH1 displayed the same key interactions as **4**, with the added benefit of adopting a nearly coplanar acetamide conformation (6° dihedral angle) and permitting a unique interaction with the backbone NH of Gly34 in the absence of a water molecule (Figure 4B).

N6 of naphthyridine **4** and N6 of tetrahydronaphthyridine **5** had significantly different pK_a values, 3.5 and 7.5, respectively, yet both compounds showed similar permeability rates at physiological pH with no efflux (AB/BA = 37/45 × 10^{-6} and 35/32 × 10^{-6} cm/s, respectively). The excellent permeability of **5**, together with an identical $logD_{7.4}$ (2.5) to its nonbasic congener **4** suggested the presence of an intramolecular hydrogen bond between protonated N6 and the acetamide carbonyl in solution (although this was not evident in a crystal structure of the hydrochloride salt (see Supporting Information)). As in the transposition of **3** to **2**, removal of the bicycle in **5** to give the aminopyridine **6** resulted in an order of magnitude loss in potency (IC_{50} = 0.33 nM). This residual potency was abolished when the pyridine core was replaced with phenyl (data not shown), demonstrating the critical role of the DMAP-like basic nitrogen in **5** and **6** and its ability to facilitate the adoption of nearly coplanar acetamide conformations via intramolecular hydrogen bonds.

In light of the unprecedented potency of tetrahydronaphthyridine **5**, we confirmed that it is a tight reversible binder ($K_{i(app)}$ = 5.2 ± 0.9 pM, K_i = 1.7 pM), and no acetylation of MTH1 was observed. The compound is chemically stable at pH 6, 7.5, and 9 at 40 °C, is unreactive with glutathione, and displays desirable kinetic solubility at pH 2 and 7 (97 and 70 μM, respectively). A preliminary screen revealed no significant affinity for kinases (S(35) = 0 at 10 μM; 97 kinase panel).[12] However, **5** was not fully stable in human and rat plasma ($t_{1/2}$ = 252 and 446 min, respectively) and predicted hepatic clearance from microsomal stability assays approached liver blood flow in human (0.89 L/h/kg) and rat (3.5 L/h/kg). Metabolite identification studies in human liver microsomes indicated deacetylation as the major metabolic pathway (72%), followed by oxidative metabolism of the resulting 7-amino-tetrahydronapthyridine.

Thus, we attempted to replace the acetamide moiety to improve metabolic stability while maintaining the Gly34 interaction (Table 1). Ureas **13** and **14** were among the most potent analogues, yet solely lowering the logD was insufficient to achieve full stability. Compounds **16**, **17**, and **3** in which the amide was replaced or absent demonstrated that reasonable stability could be achieved, albeit at the expense of potency. We also investigated *O*- and *N*-linked aryls and variously substituted alkyls in the pyrimidine-2,4-diamine series (Table 2). Compounds **19** and **21** validated that heteroatoms were tolerated in the linker, albeit with a slight loss in potency. Further optimization toward (*S*)-ethoxyphenyl analogue **23**, (*S*)-*N*-methyl-1-phenylethan-1-amine **25** (IC_{50} = 0.49 nM, LLE = 7.3), and piperidine derivatives **26**, **29**, and **30** successfully restored MTH1 IC_{50} to ≤1 nM. Although excellent biochemical potency, kinetic solubility, and permeability were achievable, this lipophilic series suffered from poor metabolic stability and was intolerant to polar and logD lowering substituents. The 2-amino and 4-methylamino groups of **1** showed little tolerance to change, emphasizing the importance of preserving optimal interactions with Asp120 and Asp119.

Our third series of small molecule MTH1 inhibitors was designed to explore interactions with Asn33 in the active site. This residue has been reported to be critical for 8-oxo-dGMP binding and specificity, interacting with both the 2-amino group and N3 of the ligand. Since the 2,4-diaminopyrimidine of **TH287** shared similar interactions, we proposed 2-aminotriazolopyridine and 2-aminobenzimidazole cores to

DOI: 10.1021/acsmedchemlett.9b00420
ACS Med. Chem. Lett. XXXX, XXX, XXX−XXX

Table 1. Acetamide Moiety Replacements in the Tetrahydronaphthyridine Series in an Attempt To Improve Metabolic Stability while Maintaining MTH1 Biochemical Potency[a]

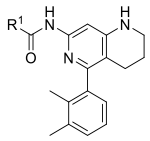

Compound	R^1	MTH1 IC_{50} (nM)	Human MS Cl (L/h/kg)
5	-NHC(O)Me	0.043	0.89
8	-NHC(O)Et	0.17	0.88
9	-NHC(O)cPr	0.06	0.38
10	-NHC(O)*i*Pr	0.61	0.73
11	-NHC(O)cBu	<0.05	0.45
12	-NHC(O)CF_2H	0.11	0.81
13	-NHC(O)NH_2	<0.05	0.33
14	-NHC(O)NHMe	<0.05	0.28
15	-NHC(O)OMe	0.15	0.39
16	-NHC(=NH)Me	62	0.18
17	-$NHSO_2$Me	773	0.11
3	-NH_2	952	0.23

[a]For number of replicates and standard error of the mean, see the Supporting Information.

interrogate their potential to interact with Asn33 and yield potent inhibitors (Table 3). We discovered that 2-amino-triazolopyridine **32** maintained good potency (MTH1 IC_{50} = 13 nM, LLE = 6.0), while the R^5 phenyl derivative **31** lost 9-fold in potency. Cocrystallization of **32** with MTH1 confirmed key hydrogen bonding interactions with Asn33, Asp119, Asp120, and an additional $\pi-\pi$ stacking interaction with Trp117 (Figure 5). Although the triazolopyridine **34** was designed to engage Asp119, the additional amino group at R^3 failed to yield a more potent compound. Acetylation of **32** resulted in a 35-fold loss in potency (data not shown), and the triazolopyridine regioisomer **40** was similarly less potent. Methylation at the R^4 position yielded the most potent compound in this series (MTH1 IC_{50} of **36** = 4.1 nM).

Triazolopyridine **32** was found to be stable in human liver microsomes (pred. hep. Cl = 0.11 L/h/kg) and moderately stable in rat liver microsomes (pred. hep. Cl = 0.86 L/h/kg). When administered to Sprague–Dawley rats at 5 mg/kg PO and 1 mg/kg IV, compound **32** showed excellent oral bioavailability (F = 86%), good *in vitro*/*in vivo* correlation (Cl = 0.73 L/h/kg), moderate volume (2.7 L/kg), and a half-life of 3.2 h. It lacks inhibition of hERG and five CYP isoforms (IC_{50} > 25 μM), while demonstrating high permeability (Caco-2 AB/BA = 41/34 × 10^{-6} cm/s) and high solubility at pH 2 and 7 (93/74 μM). In addition, it had low affinity for kinases (S(35) = 0.01 at 10 μM; 97 kinase panel) and did not activate human PXR at 15 μM. The 2-aminobenzimidazole **37** also emerged as a useful lead, with an *in vitro* MTH1 IC_{50} of 15 nM and good metabolic stability (pred. hep. Cl = 0.11 and 0.22 L/h/kg in human and rat, respectively). With three highly potent scaffolds capable of inhibiting MTH1, we then selected tool molecules **5**, **25**, **26**, **32**, and **37** to further evaluate their antiproliferative effects and ability to induce DNA damage in cancer cell lines.

To characterize the effect of these novel MTH1 inhibitors on the growth of cancer cells, we employed a 3-day cell

Table 2. MTH1 Biochemical Potencies with *O*- and *N*-Linked R^2 Groups[a]

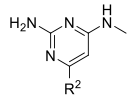

Compound	R^2	MTH1 IC_{50} (nM)
1	-2,3-diMePh	7.2
18	-OPh	6.8
19	-O-2,3-diMePh	16
20	-OBn	26
21	-NH-2,3-diMePh	40
22	-NH-cyclohexyl	12
23	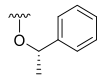	0.70
24	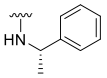	5.6
25	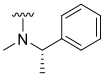	0.49
26		0.80
27		51
28		3.7
29	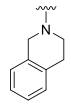	0.82
30		1.1

[a]For number of replicates and standard error of the mean, see the Supporting Information.

viability (CTG) assay in U2OS cells. We were surprised by the observation that our potent inhibitors, particularly tetrahydronaphthyridine **5** (IC_{50} = 43 pM, CTG EC_{50} = 8.0 μM, Figure 6A and Table 4), did not elicit a similar or greater antiproliferative effect than **TH287** (CTG EC_{50} = 0.7 μM). Several subsequent 3-day CTG experiments containing additional positive controls (**TH287**, **TH588**, and/or (***S***)-**crizotinib**) showed our compounds were consistently less effective than the tool compounds listed above. An *in vitro* assessment of cytotoxicity was conducted in various cell lines, and we found that **TH287** exhibited cytotoxic effects in MT4 cells (CC_{50} = 726 nM), whereas **5** and **32** showed greatly reduced cytotoxicity (CC_{50} = 19 and >50 μM, respectively).[13] Since all compounds tested had relatively similar binding in cell culture media, we hypothesized that the differential cytotoxicity could indicate that MTH1 inhibition alone was insufficient for antiproliferative activity, and we proceeded to further characterize the effect of this structurally diverse set of MTH1 inhibitors on the purported downstream markers of MTH1 inhibition.

DOI: 10.1021/acsmedchemlett.9b00420
ACS Med. Chem. Lett. XXXX, XXX, XXX−XXX

Table 3. Structural Modifications to Improve Potency in the Triazolopyridine and Benzimidazole Series[a]

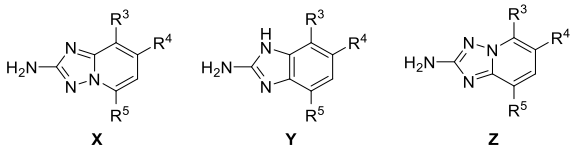

Compound	Core	R^3	R^4	R^5	MTH1 IC_{50} (nM)
31	X	H	H	Ph	936
32	X	H	H	2,3-diClPh	13
33	X	H	H	2,3-diMePh	40
34	X	NH_2	H	2,3-diClPh	207
35	X	H	Me	piperidinyl	946
36	X	H	Me	2,3-diClPh	4.1
37	Y	H	H	2,3-diClPh	15
38	Y	H	Me	2,3-diClPh	20
39	Y	H	OMe	2,3-diClPh	13
40	Z	H	H	2,3-diClPh	467

[a]For number of replicates and standard error of the mean, see the Supporting Information.

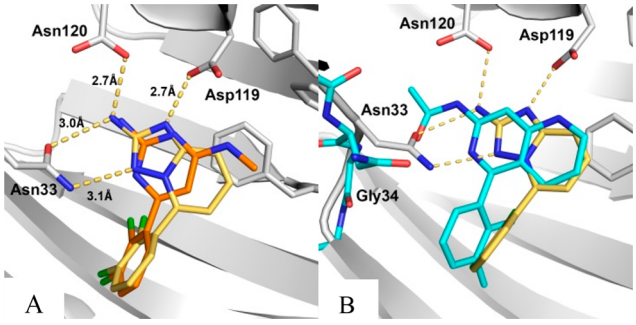

Figure 5. (A) Cocrystal structure of compound **32** (yellow) with MTH1 (1.95 Å, PDB code 6US4) and TH287 (orange) overlaid, revealing common interactions with Asn33, Asp119, and Asp120. Compound **32** also forms a $\pi-\pi$ stacking interaction with Trp117 (not shown in this figure). (B) Overlay of **5** (cyan) and **32** (yellow) showing Gly34 has moved away to allow Asn33 to interact with **32**.

Induction of DNA damage and activation of the DNA damage response pathway have been reported to be associated with inhibition of MTH1, and we interrogated both end points in cellular assays.[3] Activation of p53 in response to DNA damage has been well characterized and recently reviewed.[14] Using Simple Western, we evaluated the effect of **TH287** and several structurally diverse MTH1 inhibitors on p53 phosphorylation in U2OS cells treated for 4 and 24 h. We found that treatment with **TH287**, **TH588**, and the positive control (mitoxantrone) resulted in activation of p53, while the newly synthesized MTH1 inhibitors **5** (Figure 6B) and **32** (Supporting Information) failed to do so. As a final step to profile the cellular phenotypes of MTH1 inhibition, we used confocal microscopy to determine the extent of γH2AX foci formation in U2OS cells treated with MTH1 inhibitors. A normal cellular response to initiate DNA double-stranded break repair involves the recruitment and phosphorylation of multiple H2AX histones in close proximity to the site of repair.[15] As expected, treatment with both **TH287** and hydrogen peroxide resulted in a larger number of γH2AX foci observed in each cell nucleus (Figure 6C). However, when **5**, **32**, and **26** were tested at a concentration of 20 μM, induction of foci was not observed. Notably, these compounds

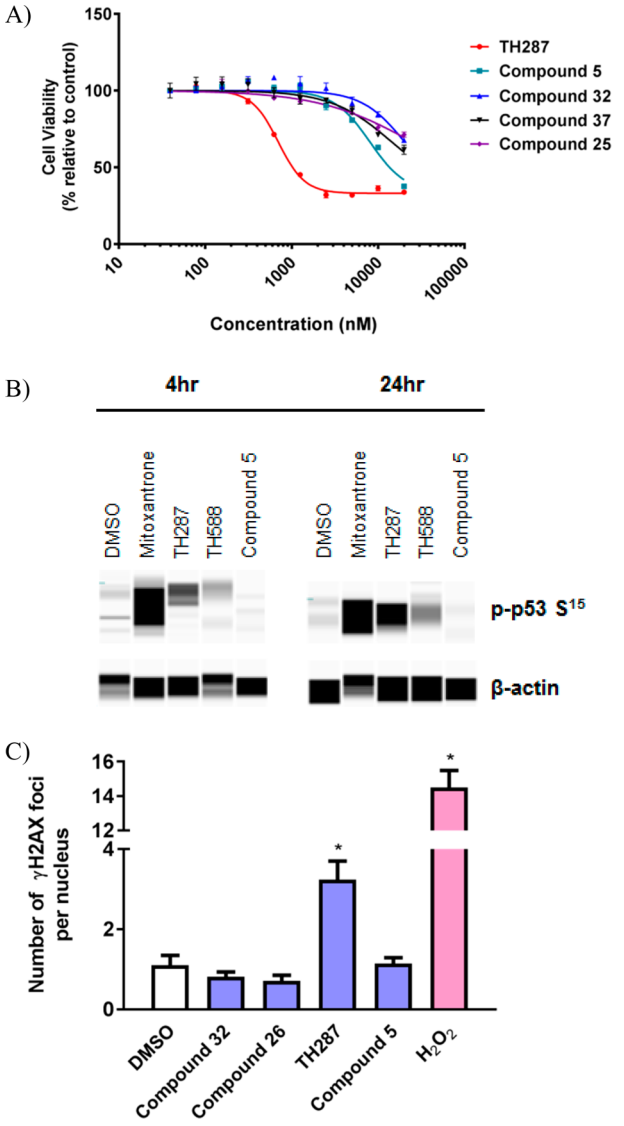

Figure 6. (A) Three-day cell viability assay in U2OS cells using CellTiter-Glo readout. (B) Expression of p-p53 and β-actin in U2OS cells treated with **TH287**, **TH588**, and compound **5** at 5 μM and mitoxantrone at 2.25 μM, measured using Peggy Sue Western blot. (C) Induction of DNA damage foci in U2OS cells with MTH1 inhibitors. Cells were incubated for 72 h with DMSO, MTH1 inhibitors (20 μM), and H_2O_2 (150 μM). Ninety to 120 nuclei were counted per experiment (*$p < 0.001$).

Table 4. MTH1 Biochemical Potencies (8-oxo-dGTP as Substrate) and Cellular Potencies (Three-day Cell Viability Assay in U2OS Cells) of Representative Tool Compounds from Our Various Chemotypes[a]

Chemotype	Compound	MTH1 IC_{50} (nM)	Cell viability EC_{50} (nM)
2,4-Diaminopyrimidine	**TH287**	4.1	699
Tetrahydronaphthyridine	**5**	0.043	8048
2,4,6-Triaminopyrimidine	**25**	0.49	24916
2-Aminotriazolopyridine	**32**	13	20323
2-Aminobenzimidazole	**37**	15	14416

[a]For number of replicates and standard error of the mean, see the Supporting Information.

DOI: 10.1021/acsmedchemlett.9b00420
ACS Med. Chem. Lett. XXXX, XXX, XXX−XXX

all demonstrated good cellular permeability and were tested in the foci formation assay at concentrations >1000-fold above their respective IC_{50} values.

Although the collective results from the cellular assays described thus far clearly show the compounds described herein failed to recapitulate the cell killing effect of previously described MTH1 inhibitors, the end points assessed are all several steps downstream, and the lack of a direct cellular readout for MTH1 inhibition hampered our ability to make definitive conclusions about the cellular activity of our series. To address this unanswered question, we developed methodology to measure the intracellular concentration of oxidized nucleoside triphosphates (oxo-NTPs), as inhibition of MTH1 was hypothesized to increase oxo-NTP levels in cells (Table 5, see the Supporting Information for methods). A large number of cells were required for this analysis as 8-oxo-dGTP and 8-oxo-rGTP levels were consistently low and near the limit of quantification. However, intracellular dGTP and rGTP concentrations remained within ranges reported in the literature.[16] U2OS cells treated with either MTH1 shRNA or representative small molecule inhibitor **37** showed no evidence of increased 8-oxo-dGTP or 8-oxo-rGTP levels *in vitro*, suggesting that MTH1 inhibition may not disrupt homeostasis of the oxo-NTP pool.

Table 5. Intracellular Concentrations of Oxo-NTPs in the Presence of Control shRNA, MTH1 shRNA, and Small Molecule MTH1 Inhibitor 37[a]

	Intracellular Concentration (pmol/million cells)			
Cell Type	8-oxo-dGTP	8-oxo-rGTP	dGTP	rGTP
SW480[b]	0.004[d]	-	6.31	2790
U2OS[c]	0.008	0.058	17.0	4370
U2OS, NT[e] shRNA	0.006	0.034	7.43	ND
U2OS, MTH1 shRNA[f]	0.010	0.022	5.58	ND
U2OS + 20 μM **37**	0.007	0.040	12.0	ND

[a] $n = 1$. [b] SW480:12 × 10^6 cells. [c] U2OS: 30 × 10^6 cells. [d] LOQ = 0.004 pmol/million cells. [e] Nontargeting (NT). [f] About 50% knockdown when harvested.

In this study, the validity of MTH1 as an oncology target was assessed by the discovery and characterization of structurally diverse chemotypes in conjunction with specific assessment of cellular effects. Despite nano- and subnanomolar potencies, the tool compounds did not elicit the desired antiproliferative effects, failed to induce p53 activation, and did not increase foci formation or 8-oxo-dGTP levels in U2OS cells, leading us to conclude that MTH1 alone is insufficient for cancer cell death.[17,18] During the months following the conclusion of our MTH1 efforts, several articles, perspectives, and comments were published corroborating our findings. The use of dissimilar chemotypes for phenotypic confirmation was evident in many of these programs and can be a valuable tactic at an early stage of a project. Publication of efforts such as these furthers our collective understanding of methods for *in vitro* target validation.

■ ASSOCIATED CONTENT

Supporting Information

The Supporting Information is available free of charge on the ACS Publications website at DOI: 10.1021/acsmedchemlett.9b00420.

Synthetic procedures and characterization of MTH1 inhibitors, small molecule X-ray structures of **4** and **5**, MTH1 crystallography, data collection and refinement statistics, kinase selectivity profile, biochemical and cellular assay protocols, and intracellular measurements of oxo-NTPs (PDF)

Accession Codes

Cocrystal structures of MTH1 with **4**, **5** and **32** have been deposited with the Protein Data Bank under Accession ID codes 6US3, 6US2 and 6US4.

■ AUTHOR INFORMATION

Corresponding Author

*E-mail: julie.farand@gilead.com. Phone: +1-650-372-7668.

ORCID

Julie Farand: 0000-0001-9991-4328

Brian E. Schultz: 0000-0001-9757-2547

Eric B. Lansdon: 0000-0001-9461-1475

Author Contributions

The manuscript was written through the contributions of all authors. All authors have given approval to the final version of the manuscript.

Notes

The authors declare no competing financial interest.

■ ACKNOWLEDGMENTS

The authors would like to thank the staff at the Advanced Light Source for help in data collection. The Advanced Light Source is a Department of Energy Office of Science User Facility under Contract No. DE-AC02-05CH11231. The authors also wish to thank Professor Arnold L. Rheingold for providing small molecule X-ray crystallography data.

■ ABBREVIATIONS

FDA, Food and Drug Administration; 8-oxo-dGMP, 8-oxo-2′-deoxyguanosine-5′-monophosphate; dNTP, deoxynucleoside triphosphate; shRNA, short hairpin ribonucleic acid; Asp, aspartic acid; Asn, asparagine; Trp, tryptophan; Gly, glycine; LLE, lipophilic ligand efficiency; DMAP, 4-dimethylaminopyridine; PXR, pregnane X receptor

■ REFERENCES

(1) Novel Drug Approvals for 2018. https://www.fda.gov/drugs/new-drugs-fda-cders-new-molecular-entities-and-new-therapeutic-biological-products/novel-drug-approvals-2018 (accessed September 12, 2019).

(2) Mullard, A. 2018 FDA Drug Approvals. *Nat. Rev. Drug Discovery* **2019**, *18*, 85−89.

(3) Gad, H.; Koolmeister, T.; Jemth, A. S.; Eshtad, S.; Jacques, S. A.; Ström, C. E.; Svensson, L. M.; Schultz, N.; Lundbäck, T.; Einarsdottir, B. O.; Saleh, A.; Göktürk, C.; Baranczewski, P.; Svensson, R.; Berntsson, R. P.; Gustafsson, R.; Strömberg, K.; Sanjiv, K.; Jacques-Cordonnier, M. C.; Desroses, M.; Gustavsson, A. L.; Olofsson, R.; Johansson, F.; Homan, E. J.; Loseva, O.; Bräutigam, L.; Johansson, L.; Höglund, A.; Hagenkort, A.; Pham, T.; Altun, M.; Gaugaz, F. Z.; Vikingsson, S.; Evers, B.; Henriksson, M.; Vallin, K. S.; Wallner, O. A.; Hammarström, L. G.; Wiita, E.; Almlöf, I.; Kalderén, C.; Axelsson, H.; Djureinovic, T.; Puigvert, J. C.; Häggblad, M.; Jeppsson, F.; Martens, U.; Lundin, C.; Lundgren, B.; Grenelli, I.; Jensen, A. J.; Artursson, P.; Nilsson, J. A.; Stenmark, P.; Scobie, M.; Berglund, U. W.; Helleday, T. MTH1 Inhibition Eradicates Cancer by Preventing Sanitation of the dNTP pool. *Nature* **2014**, *508*, 215−221.

DOI: 10.1021/acsmedchemlett.9b00420
ACS Med. Chem. Lett. XXXX, XXX, XXX−XXX

(4) Huber, K. V.; Salah, E.; Radic, B.; Gridling, M.; Elkins, J. M.; Stukalov, A.; Jemth, A. S.; Göktürk, C.; Sanjiv, K.; Strömberg, K.; Pham, T.; Berglund, U. W.; Colinge, J.; Bennett, K. L.; Loizou, J. I.; Helleday, T.; Knapp, S.; Superti-Furga, G. Stereospecific Targeting of MTH1 by (*S*)-Crizotinib as an Anticancer Strategy. *Nature* **2014**, *508*, 222−227.
(5) Curtin, N. J. DNA Repair Dysregulation from Cancer Driver to Therapeutic Target. *Nat. Rev. Cancer* **2012**, *12*, 801−817.
(6) Streib, M.; Kräling, K.; Richter, K.; Xie, X.; Steuber, H.; Meggers, E. An Organometallic Inhibitor for the Human Repair Enzyme 7,8-Dihydro-8-oxoguanosine Triphosphatase. *Angew. Chem., Int. Ed.* **2014**, *53*, 305−309.
(7) Kettle, J.; Alwan, H.; Bista, M.; Breed, J.; Davies, N. L.; Eckersley, K.; Fillery, S.; Foote, K. M.; Goodwin, L.; Jones, D. R.; Kack, H.; Lau, A.; Nissink, J. W. M.; Read, J.; Scott, J. S.; Taylor, B.; Walker, G.; Wissler, L.; Wylot, M. Potent and Selective Inhibitors of MTH1 Probe Its Role in Cancer Cell Survival. *J. Med. Chem.* **2016**, *59*, 2346−2361.
(8) Petrocchi, A.; Leo, E.; Reyna, N.; Hamilton, M. M.; Shi, X.; Parker, C. A.; Mseeh, F.; Bardenhagen, J. P.; Leonard, P.; Cross, J. B.; Huang, S.; Jiang, Y.; Cardozo, M.; Draetta, G.; Marszalek, J. R.; Toniatti, C.; Jones, P.; Lewis, R. T. Identification of Potent and Selective MTH1 Inhibitors. *Bioorg. Med. Chem. Lett.* **2016**, *26*, 1503−1507.
(9) Kawamura, T.; Kawatani, M.; Muroi, M.; Kondoh, Y.; Futamura, Y.; Aono, H.; Tanaka, M.; Honda, K.; Osada, H. Proteomic Profiling of Small-Molecule Inhibitors Reveals Dispensability of MTH1 for Cancer Cell Survival. *Sci. Rep.* **2016**, *6*, 26521.
(10) Ellermann, M.; Eheim, A.; Rahm, F.; Viklund, J.; Guenther, J.; Andersson, M.; Ericsson, U.; Forsblom, R.; Ginman, T.; Lindström, J.; Silvander, C.; Trésaugues, L.; Giese, A.; Bunse, S.; Neuhaus, R.; Weiske, J.; Quanz, M.; Glasauer, A.; Nowak-Reppel, K.; Bader, B.; Irlbacher, H.; Meyer, H.; Queisser, N.; Bauser, M.; Haegebarth, A.; Gorjánácz, M. Novel Class of Potent and Cellularly Active Inhibitors Devalidates MTH1 as Broad-Spectrum Cancer Target. *ACS Chem. Biol.* **2017**, *12*, 1986−1992.
(11) Svensson, L. M.; Jemth, A.-S.; Desroses, M.; Loseva, O.; Helleday, T.; Högbom, M.; Stenmark, P. Crystal Structure of Human MTH1 and the 8-Oxo-dGMP Product Complex. *FEBS Lett.* **2011**, *585*, 2617−2621.
(12) DiscoverX kinase selectivity score S(35) = (number of nonmutant kinases with % control < 35)/(number of nonmutant kinases tested).
(13) Feng, J. Y.; Xu, Y.; Barauskas, O.; Perry, J. K.; Ahmadyar, S.; Stepan, G.; Yu, H.; Babusis, D.; Park, Y.; McCutcheon, K.; Perron, M.; Schultz, B. E.; Sakowicz, R.; Ray, A. S. Role of Mitochondrial RNA Polymerase in the Toxicity of Nucleotide Inhibitors of Hepatitis C Virus. *Antimicrob. Agents Chemother.* **2016**, *60*, 806−817.
(14) Williams, A. B.; Schumacher, B. p53 in the DNA-Damage-Repair Process. *Cold Spring Harbor Perspect. Med.* **2019**, *6*, a026070.
(15) Nakamura, A. J.; Rao, V. A.; Pommier, Y.; Bonner, W. M. The Complexity of Phosphorylated H2AX Foci Formation and DNA Repair Assembly at DNA Double-Strand Breaks. *Cell Cycle* **2010**, *9*, 389−397.
(16) Traut, T. W. Physiological Concentrations of Purines and Pyrimidines. *Mol. Cell. Biochem.* **1994**, *140*, 1−22.
(17) Papeo, G. MutT Homolog 1 (MTH1): The Silencing of a Target. *J. Med. Chem.* **2016**, *59*, 2343−2345.
(18) Einarsdottir, B. O.; Karlsson, J.; Söderberg, E. M. V.; Lindberg, M. F.; Funck-Brentano, E.; Jespersen, H.; Brynjolfsson, S. F.; Olofsson Bagge, R.; Carstam, L.; Scobie, M.; Koolmeister, T.; Wallner, O.; Stierner, U.; Warpman Berglund, U.; Ny, L.; Nilsson, L. M.; Larsson, E.; Helleday, T.; Nilsson, J. A. A Patient-Derived Xenograft Pre-Clinical Trial Reveals Treatment Responses and a Resistance Mechanism to Karonudib in Metastatic Melanoma. *Cell Death Dis.* **2018**, 810.

DOI: 10.1021/acsmedchemlett.9b00420
ACS Med. Chem. Lett. XXXX, XXX, XXX−XXX